aerospace

MDPI

Article

A Design Method for Elliptical Orbit Constellations Targeting Discontinuous Regional Coverage in Environmental Monitoring

Yi Wei and Zhanxia Zhu *

National Key Laboratory of Aerospace Flight Dynamics, College of Astronautics, Northwestern Polytechnical University, Xi'an 710072, China; saywy@mail.nwpu.edu.cn
* Correspondence: zhuzhanxia@nwpu.edu.cn

Abstract

Satellite constellations are increasingly employed in regional remote sensing applications such as environmental monitoring and disaster management. However, achieving efficient and timely coverage for discontinuous regions with high revisit frequency remains a significant challenge. This study first compares low Earth circular and elliptical orbit constellations in terms of coverage performance, economic efficiency, and orbital lifetime. Based on this comparison, a dedicated design methodology for elliptical orbit constellations aimed at discontinuous regional coverage is developed. A critical Sun-synchronous repeating elliptical orbit is selected as the baseline configuration, and its key orbital parameters including the semi-major axis, eccentricity, and argument of perigee are analytically derived. Furthermore, a flexible constellation configuration model is proposed, introducing a modified Walker-inspired $kn/kn/k$ pattern. This model establishes direct mathematical relationships between the constellation's repetition factor, phasing parameters, and temporal coverage metrics to systematically guide the overall design process. A case study on wildfire monitoring in China's Qinling Mountains demonstrates the feasibility and effectiveness of the proposed approach, achieving a one-hour revisit time over the target region with a 24-satellite constellation. The results indicate that the proposed methodology provides a cost-effective and adaptable framework for satellite constellation design in remote sensing applications, particularly suited to dynamic environmental monitoring and emergency response missions.

Keywords: elliptical orbit; satellite constellation; discontinuous regional coverage; revisit time; wildfire

Check for updates

Academic Editor: Hyun-Ung Oh

Received: 12 March 2026
Revised: 9 April 2026
Accepted: 13 April 2026
Published: 14 April 2026

Copyright: © 2026 by the authors. Licensee MDPI, Basel, Switzerland. This article is an open access article distributed under the terms and conditions of the Creative Commons Attribution (CC BY) license.

1. Introduction

Satellite constellations have been widely used in various fields such as communications, remote sensing, and navigation [1–3]. It is well known that the constellations can fall into various categories depending on the type of coverage (continuous/discontinuous), the type of coverage region (global/regional), the type of orbit (circular/elliptical/hybrid), and the altitude of implementation (low/medium/geosynchronous Earth orbit) [4]. In this paper, we are focused on elliptical orbit and discontinuous regional coverage constellations, which are often used for monitoring and reconnaissance of the region of interest. A region of interest can be defined as an area where ground observation is often required owing to the high density of military threats or frequent occurrence of national disasters [5].

Circular-orbit constellations have been extensively studied, and several classical design frameworks, such as Walker constellations and Streets-of-Coverage (SOC) constellations,

have been established [6,7]. These configurations are effective for global or near-global coverage because satellites are regularly distributed over multiple orbital planes. However, such globally symmetric structures are often inefficient for regional observation missions, especially when the target areas are spatially discontinuous. In these cases, a considerable portion of the observation resources may be spent over non-target regions, resulting in reduced coverage efficiency and increased revisit time over the areas of interest [8]. This issue is particularly critical in applications such as disaster monitoring and environmental surveillance, where rapid revisit capability is essential for timely response [9].

To improve regional adaptability, several studies have extended or modified traditional Walker-type ideas. Representative examples include flower constellations, necklace-based configuration methods, and other restricted repeating-ground-track patterns, which improve the spatial–temporal matching between orbital motion and mission-driven coverage demand [10–14]. These developments indicate that constellation design is increasingly shifting from globally uniform patterns toward more flexible mission-oriented architectures. Nevertheless, most existing adaptations are still mainly developed for circular or near-circular orbits, and a dedicated analytical configuration framework for discontinuous regional coverage under elliptical orbits remains limited.

In parallel, optimization-based constellation design methods have also become increasingly important. By directly linking constellation geometry with performance metrics such as coverage and revisit time, these methods can explore large design spaces more flexibly than purely analytical approaches. For example, Deccia et al. [15] employed a multiobjective genetic algorithm to design satellite constellations for recovering Earth system mass change. Although their application focuses on gravity recovery, the underlying optimization framework is directly relevant to regional coverage design. Compared with such approaches, analytical methods generally offer clearer physical interpretability and lower computational burden, whereas optimization methods provide stronger design-space exploration capability and potentially better trade-offs in solution quality. Therefore, the present work is positioned as a dedicated analytical design framework that complements, rather than replaces, optimization-based approaches.

Several studies have also specifically addressed discontinuous or region-constrained coverage problems. Razoumny's route constellation concept demonstrated excellent performance and even outperformed the best Walker constellations in certain discontinuous coverage scenarios [16]. Sarno et al. proposed a polar constellation design based on SOC theory to improve revisit performance in polar regions [17]. Other researchers have investigated repeating-ground-track-based regional coverage methods [18], constellation design for multi-area IoT services [19], and matheuristic approaches for regional constellation optimization [20]. Although these studies have enriched the constellation design landscape, challenges remain in balancing generality, physical interpretability, and computational tractability.

To overcome the limitations of circular-orbit systems in regional observation, highly elliptical orbits (HEOs) have attracted growing attention. Unlike circular orbits, elliptical orbits allow satellites to remain longer over specific regions during each orbital period, thereby increasing dwell time and improving revisit performance. The Molniya orbit is a classical example that provides prolonged visibility over high-latitude regions poorly served by geostationary satellites [21]. More recently, elliptical Sun-synchronous repeating orbits have been explored for regional optical remote sensing because they combine prolonged regional visibility with relatively stable illumination conditions [22]. However, despite these advantages, constellation design methods for elliptical orbits remain less mature than those for circular orbits. In particular, for discontinuous regional targets,

the coupling among orbit repetition characteristics, constellation phasing, and revisit-time requirements has not yet been formulated in a sufficiently systematic manner.

This paper proposes a systematic design methodology for elliptical orbit constellations tailored to discontinuous regional coverage. The approach analytically derives key orbital parameters such as semi-major axis, eccentricity, and argument of perigee for a critical Sun-synchronous repeating orbit. A configuration pattern is then established that links constellation parameters with coverage metrics, enabling efficient design for regional revisit requirements. The methodology is demonstrated through a case study of wildfire monitoring in China's Qinling Mountains, a representative scenario with rugged terrain and spatially scattered fire risk zones. The results show that the designed 24-satellite elliptical constellation can achieve a 1 h revisit requirement over the region of interest, while a circular-orbit Walker benchmark with the same number of satellites fails to satisfy this requirement, thereby verifying the advantage of the proposed framework for discontinuous regional coverage missions.

The remainder of this paper is organized as follows. Section 2 compares circular and elliptical constellations for discontinuous regional observation in terms of coverage performance, economic efficiency, and orbital lifetime. Section 3 presents the nominal orbit design procedure for the proposed elliptical constellation. Section 4 introduces the corresponding constellation configuration design method. Section 5 provides a simulation case study for wildfire monitoring in the Qinling Mountains. Finally, Section 6 concludes the paper.

2. Comparison Between Circular Orbit Constellations and Elliptical Orbit Constellations

Regarding the satellite constellation design for discontinuous regional observation missions, this section will evaluate and compare the performance of circular orbit constellations and elliptical orbit constellations from three aspects: orbit lifetime, economic performance and coverage performance.

2.1. Comparison of Constellation Orbit Lifetime

King-Hele's classical monograph "Satellite Orbits in an Atmosphere: Theory and Application" [23] provides an analytical treatment of low-Earth satellite motion under atmospheric drag and Earth's oblateness, and has long served as a fundamental reference for orbital lifetime prediction and drag-perturbed orbit theory. In remote sensing missions, especially for high-resolution Earth observation, low-altitude orbits are often preferred due to their ability to capture finer details and provide higher spatial resolution. However, low perigee altitudes, typical of circular orbits, come with a tradeoff: the closer the orbit to the Earth's surface, the shorter the orbital lifetime due to increased atmospheric drag. The drag acceleration experienced by a satellite due to atmospheric drag can be expressed as follows [24]:

$$\bar{a}_{\text{drag}} = -\frac{1}{2} c_D \frac{A}{m} \rho \cdot v^2 \frac{\bar{v}}{|\bar{v}|} \tag{1}$$

where $\bar{a}_{\text{drag}}$ is the drag acceleration vector, c_D is the atmospheric drag coefficient of the satellite, A is the area of the satellite subject to atmospheric resistance, m is the mass of the satellite, ρ is the atmospheric density, and v is the relative velocity between the atmospheric and satellite. In this study, the drag coefficient is taken to be 2.2, the satellite's area to 2 m^2 and its mass to 100 kg. The Jacchia-Roberts model was applied to predict the lifetime of a satellite. Figure 1 illustrates this effect for circular orbits, where the semi-major axis decreases over time as the orbit decays. Circular orbits at 300 km and 400 km perigee experience rapid decay, with their lifetimes limited to just 1–2 years due to the strong drag

at low altitudes. For remote sensing tasks that require frequent observations, such short lifetimes present significant challenges in satellite operations and system sustainability.

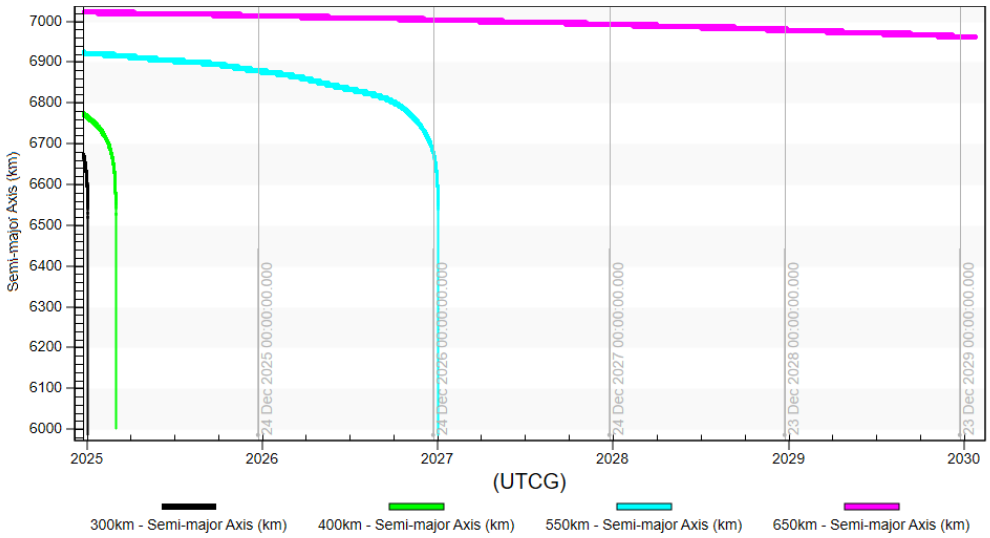


Figure 1. Semi-major axis evolution of circular orbits with varying altitudes (300 km to 650 km).

In contrast, elliptical orbits behave differently due to the asymmetry between apogee and perigee altitudes. Figure 2 shows the variation in perigee and apogee altitudes over time for a representative elliptical orbit. The perigee altitude (green line) gradually increases, while the apogee altitude (black line) decreases. This reflects the classic orbital circularization process caused by atmospheric drag concentrated near the low-altitude perigee. In this way, elliptical orbits can provide a better balance between low-altitude observation for high-resolution imaging and longer orbital lifetimes. By adjusting the semi-major axis and perigee altitude, we can create an orbit that provides extended operational lifetimes without sacrificing the low-altitude observational capabilities critical for remote sensing.

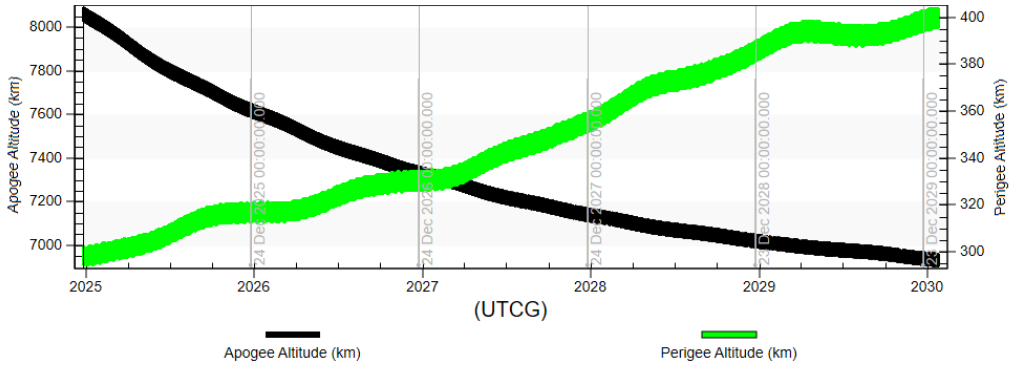


Figure 2. Time evolution of perigee and apogee altitudes for a representative elliptical orbit.

In summary, elliptical orbits offer distinct advantages over circular orbits in remote sensing missions that require both high-resolution imaging (enabled by low perigee) and long satellite lifetimes (achieved through high apogee). This combination of traits allows elliptical orbits to deliver better performance for regional or targeted observations, especially in time-critical applications such as disaster monitoring or environmental surveillance.

2.2. Comparison of Constellation Economic Performance

The performance of satellite constellations in terms of ΔV is a fundamental economic consideration, directly affecting both the propellant mass and the total cost of the mis-

sion. The required velocity change, ΔV, governs the launch, station-keeping, and reentry operations of the satellite, and is a critical parameter for determining the satellite's fuel consumption and lifetime.

The propellant mass m_p, the rocket equation to determine the total required spacecraft plus the propellant mass, $m_i = m_0 + m_p$, in terms of the dry mass of the spacecraft, m_0, the total required and the propellant exhaust velocity, ΔV [25].

$$m_i = m_0 e^{(\Delta V / V_0)} = m_0 e^{\left(\Delta V / I_{sp} g\right)} \tag{2}$$

where the specific impulse, $I_{sp} = V_0/g$, V_0 is the exhaust velocity and g is the standard gravitational acceleration, taken as $g = 9.80665\ \text{m/s}^2$. Typical exhaust velocities for chemical propellants are in the range of 2 to 4 km/s and up to 30 km/s for electric propulsion systems. The fundamental equations for the Hohmann transfer are as follows [25]:

$$a_T = \frac{1}{2}(a_L + a_H) \tag{3}$$

$$\Delta V_L = \sqrt{\mu}\left[\left(\left(\frac{2}{a_L} - \frac{1}{a_T}\right)\right)^{1/2} - \left(\left(\frac{1}{a_L}\right)\right)^{1/2}\right] \tag{4}$$

$$\Delta V_H = \sqrt{\mu}\left[\left(\left(\frac{1}{a_H}\right)\right)^{1/2} - \left(\left(\frac{1}{a_H} - \frac{1}{a_T}\right)\right)^{1/2}\right] \tag{5}$$

where a is the semi-major axis, ΔV is the change in velocity, μ is the Earth's gravitational parameter, and the subscripts L, H, and T refer to the lower circular orbit, higher circular orbit, and Hohmann transfer orbit, respectively. Because the plane change is simply a vector sum, we can determine the total ΔV required as a function of the initial and final velocities as follows:

$$\Delta V = \left(\left(V_i^2 + V_f^2 - 2V_i V_f cos\theta\right)\right)^{1/2} \tag{6}$$

where V_i is the initial velocity, V_f is the final velocity, and θ is the required angular change. The $\Delta V_{deorbit}$ required for a satellite to drop from an initial circular altitude to a reentry perigee altitude is given by

$$\Delta V_{deorbit} \approx V\left[1 - \sqrt{\frac{2(R_E + H_e)}{2R_E + H_e + H_i}}\right] \approx V\left[\frac{0.5(H_i - H_e)}{2R_E + H_i + H_e}\right] \tag{7}$$

where V is the initial satellite velocity, H_i is the initial circular altitude, H_e is the reentry perigee altitude, and R_E is the radius of the Earth. The simulation results shown in Figures 3 and 4 illustrate the ΔV required for launch and reentry for both circular and elliptical orbits. Figure 3 shows the ΔV change for a circular orbit satellite with an altitude of 350 km to 1000 km and a reentry orbit of 75 km altitude. The total ΔV increases significantly with altitude due to the higher velocities required at higher altitudes.

Figure 4 shows the ΔV change for an elliptical orbit satellite with a perigee set at 300 km, an apogee ranging from 1000 km to 10,000 km, and a reentry orbit altitude of 75 km. The ΔV for elliptical orbits shows a less steep increase with higher apogees, demonstrating that elliptical orbits can extend satellite lifetime while minimizing the ΔV required for reentry and orbital maneuvers.

Compared with circular orbits, suitably designed elliptical frozen orbits can provide potential advantages in terms of ΔV requirements for station-keeping and lifetime maintenance, which may translate into operational benefits such as reduced propellant consumption. A detailed assessment of launch and operational costs, however, is beyond the scope of this paper. By optimizing the perigee and apogee of an elliptical orbit, satellites

can reduce maintenance ΔV and extend operational lifetimes. In contrast, circular orbits at low altitudes require frequent station-keeping maneuvers due to the strong atmospheric drag, increasing fuel consumption and operating costs.

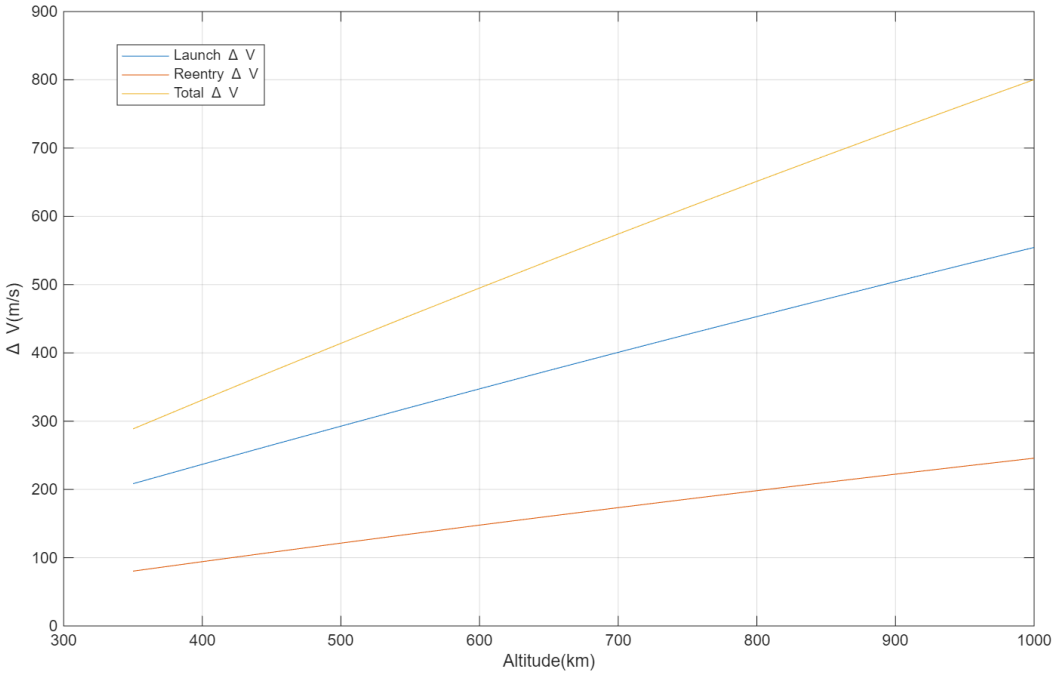


Figure 3. The ΔV change for a circular orbit satellite with an altitude of 350 km to 1000 km and a reentry orbit of 75 km altitude.

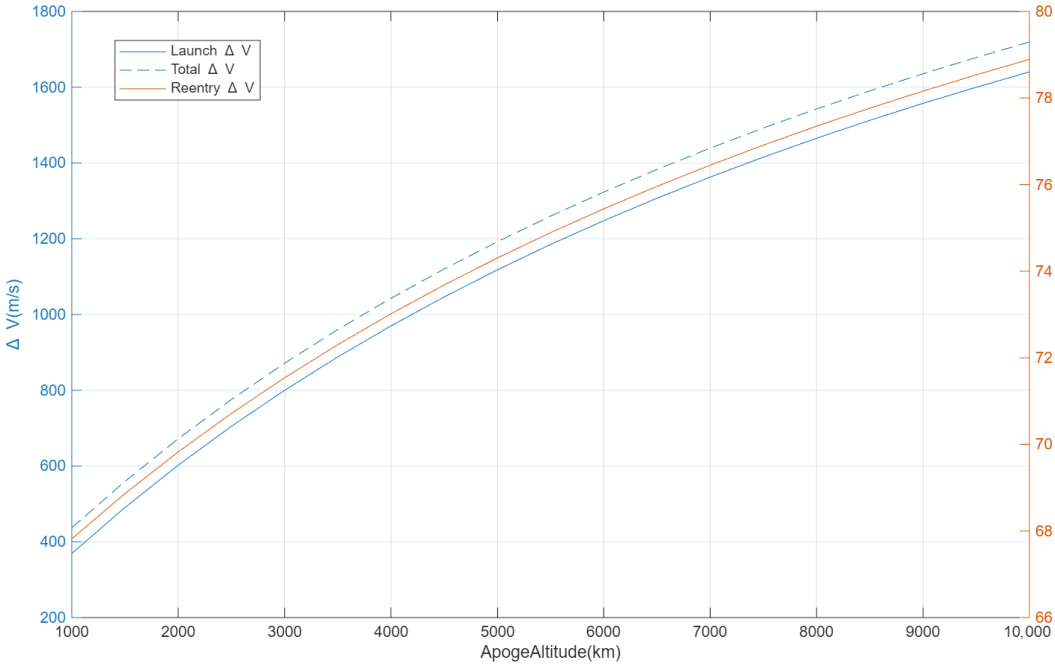


Figure 4. The ΔV change for an elliptical orbit satellite with a perigee set at 300 km, an apogee ranging from 1000 km to 10,000 km, and a reentry orbit altitude of 75 km.

In addition, elliptical orbits minimize the need for frequent station-keeping maneuvers by placing the satellite in a frozen orbit with a critical inclination, which reduces perigee drift and ultimately lowers the overall maintenance costs. This advantage is especially significant for long-term missions, where the economic burden of maintaining a circular orbit becomes substantial.

2.3. Comparison of Constellation Coverage Performance

Effective coverage is crucial for satellite constellations, especially when tasked with observing discontinuous regions or specific high-priority zones. The choice between circular and elliptical orbits directly impacts the satellite's coverage efficiency, observation time, and ability to meet mission requirements.

Circular orbits are commonly used for global coverage, where the satellite maintains a constant altitude throughout its orbit. This symmetry ensures uniform coverage over the Earth's surface, which is beneficial for applications like global climate monitoring or communications. However, this uniformity is a limitation in regional observation tasks, especially when targeting specific areas. In remote sensing, lower orbital altitudes provide higher resolution but suffer from the trade-off between coverage duration and revisit times.

For example, circular orbits with 300 km or 400 km perigee (polar orbits) provide high-resolution imaging but short lifespans due to strong atmospheric drag at low altitudes. While circular orbits are suitable for broad coverage, they require many satellites to achieve sufficient revisit frequency for a specific region, making them inefficient for discontinuous coverage.

One of the key advantages of elliptical orbits is their ability to achieve high coverage efficiency with fewer satellites compared to circular orbits. Circular orbits require multiple satellites to achieve a global or regional coverage, while elliptical constellations can achieve similar coverage with fewer satellites, by leveraging multiple elliptical orbits with slightly phased perigees. This efficiency is enhanced by adjusting the apogee to ensure that the satellites spend more time near the target region.

In applications such as wildfire monitoring, where timely observations are critical, the combination of low-perigee observation for high resolution and high-apogee orbital decay for extended lifetime, makes elliptical orbits an efficient solution. By carefully configuring the semi-major axis and perigee, revisit times can be minimized, and target region observation can be maximized.

In the coverage analysis, the Earth is modelled in an Earth-fixed frame and the coverage is computed using the STK 11 built-in coverage tool. A ground point is considered visible if its slant range to the satellite does not exceed the maximum operating range of the sensor, which is set to 500 km, and it lies inside the payload field of view. The payload is modelled as a nadir-pointing conical sensor with a half-cone angle of 45°, which defines the instantaneous ground footprint. The coverage metrics shown in the figures are computed based on this coverage model. Due to the large altitude variation along the elliptical orbit, the instantaneous observation geometry of the nadir-pointing conical sensor changes continuously. In this study, the sensor is characterized by a half-cone angle of 45° and a maximum observation range of 500 km. Under this constraint, the satellite can provide effective observation only when it is located within a limited orbital arc near perigee, where the satellite altitude satisfies the sensor-range requirement. As the satellite moves toward the high-altitude portion of the orbit, especially near apogee, the distance between the satellite and the Earth's surface exceeds the maximum allowable sensing range, and thus no effective regional coverage can be achieved. Therefore, the observation capability of the proposed elliptical orbit constellation is concentrated in the low-altitude segment around perigee, which is also the key mechanism exploited in this design to improve regional revisit performance. Accordingly, the effective observation duration in each orbital period is limited, and the regional coverage performance is determined primarily by the distribution and repetition characteristics of these usable near-perigee observation arcs.

3. Design of the Nominal Orbit for Discontinuous Regional Coverage

In satellite constellation design, the satellite orbit parameters and constellation configuration parameters jointly determine the final configuration of the satellite constellation, playing a crucial role in the coverage performance and stability of the constellation [26].

The orbit of a satellite is defined by a set of six classical orbital elements, typically categorized into two groups: orientation elements and geometric shape parameters. The orientation parameters—inclination (i), argument of perigee (ω), right ascension of the ascending node (RAAN, Ω), and true anomaly—determine the spatial orientation of the satellite relative to Earth. The geometric shape parameters—semi-major axis (a) and eccentricity (e)—define the size and shape of the orbital trajectory.

In this study, an elliptical orbit is employed as the nominal orbit for designing a constellation aimed at discontinuous regional coverage. This section presents a systematic procedure for determining each orbital parameter of the reference orbit [27].

3.1. Determination of Orbit Inclination i

For satellites in elliptical orbits, the imaging resolution across the ground track is non-uniform due to altitude variation. Moreover, orbital perturbations, particularly from Earth's oblateness (J_2) and pear-shape asymmetry (J_3), induce secular changes in orbital parameters such as eccentricity and argument of perigee. To ensure consistent imaging resolution and maintain stable orbital geometry over time, a frozen orbit is preferred—i.e., one where both $\dot{e} = 0$ and $\dot{\omega} = 0$. Under J_2 and J_3 perturbations, the variation rates of eccentricity and argument of perigee are expressed as follows:

$$\dot{e} = \frac{3nJ_3R_e^3\sin(i)}{4a^3(1-e^2)^2}\left(\frac{5}{2}\sin^2(i) - 2\right)\cos(\omega) \tag{8}$$

$$\dot{\omega} = \frac{3nJ_2R_e^3}{2a^2(1-e^2)^2}\left(\frac{5}{2}\sin^2(i) - 2\right) \tag{9}$$

In deriving the frozen-orbit conditions, we retain the zonal harmonics J_2 and J_3. The J_3 term is included because it is responsible for the long-period variation of the eccentricity vector and thus for the existence of a non-zero frozen eccentricity. Higher-order terms such as J_4 mainly provide small corrections to the J_2-dominated secular rates and do not significantly shift the frozen-orbit solution at the altitudes considered here.

The critical inclination condition $\frac{5}{2}\sin^2(i) - 2 = 0$ yields two solutions: $i = 63.43^\circ$ and $i = 116.57^\circ$. These are referred to as critical inclinations, which minimize secular drift in ω and result in a frozen elliptical orbit. To satisfy both frozen orbit conditions and ensure consistent Sun illumination, a retrograde Sun-synchronous orbit is selected. Thus, the inclination is set to $i = 116.57^\circ$.

Figure 5 illustrates the variation in the argument of perigee over 36 h for elliptical orbits with and without the critical inclination. The orbital inclination angles were set to 63.4° and 55° in an elliptical orbit with a perigee altitude of 300 km and an apogee altitude of 8000 km. The orbital motion is propagated using STK with the same perturbation and drag model as in Figures 1 and 2. The black curve corresponds to the orbit with the critical inclination of 63.4°, where the argument of perigee remains nearly constant because the J_2-induced secular drift is canceled. The green curve represents the non-critical inclination case, showing a gradual increase in the argument of perigee over time due to the unbalanced perturbation effect of the Earth's oblateness.

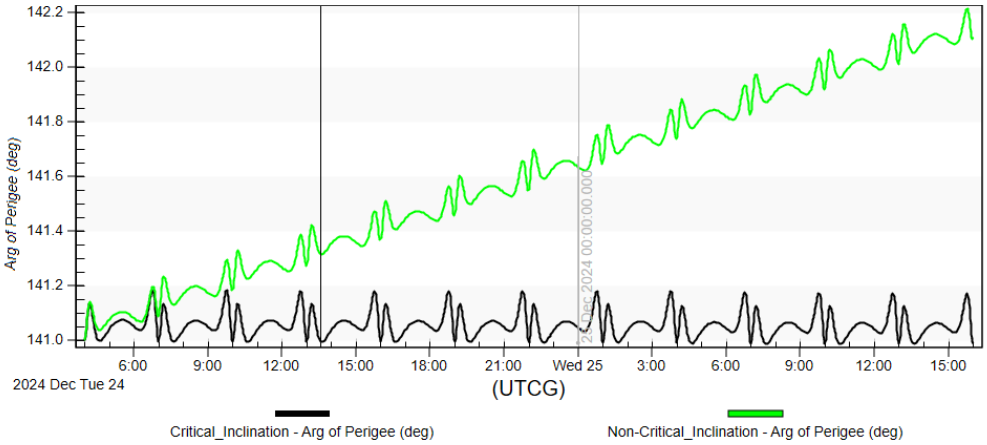


Figure 5. Temporal variation of the argument of perigee for orbit with critical and non-critical inclinations (black line: critical inclination, green line: non-critical inclination).

3.2. Determination of the Argument of Perigee ω

To maximize imaging resolution over the target region, the perigee of the elliptical orbit is positioned directly above it. Based on the target latitude δ and the selected inclination i, the argument of perigee ω can be derived using spherical geometry:

$$\sin(\delta) = \sin(\omega)\ \sin(i) \tag{10}$$

Solving for ω provides the necessary perigee orientation aligned with the mission's geographic focus.

3.3. Determination of the Eccentricity e and the Semi-Major Axis a

First, determine the perigee altitude based on mission requirements, resolution demands, and the characteristics of the imaging payload. Next, derive the semi-major axis of the orbit according to the properties of the Sun-synchronous orbit. The conditions for achieving a Sun-synchronous orbit can be derived from the Earth's orbital angular velocity around the Sun and the mean perturbation angular velocity of the orbital plane drift, as shown in the following equation:

$$\cos(i) = -0.09892\left(\frac{a}{R_e}\right)^{7/2}\left(1-e^2\right)^2 \tag{11}$$

where R_e is the Earth's equatorial radius, e is the orbital eccentricity, and they satisfy the following relationship with the semi-major axis a:

$$e = \frac{a-\left(R_e+H_p\right)}{a} \tag{12}$$

From the equation above, the semi-major axis a and orbital eccentricity e can be determined.

By leveraging the repeating ground track orbit characteristics, optimize the semi-major axis a to determine the apogee altitude H_a. A repeating ground track orbit features a repeating satellite point trajectory, enabling the satellite to retrace its path at specific time intervals and revisit any ground target within designated time frames. The repeating ground track is particularly useful for observing regions with shorter periodic interval. By using the semi-major axis derived earlier, the orbital period can be determined, which in turn defines the revisit cycle (i.e., the number of revolutions per day required for the satellite to retrace its ground track). The Figure 6 illustrates the ground track of a repeat orbit with eight revolutions per day.

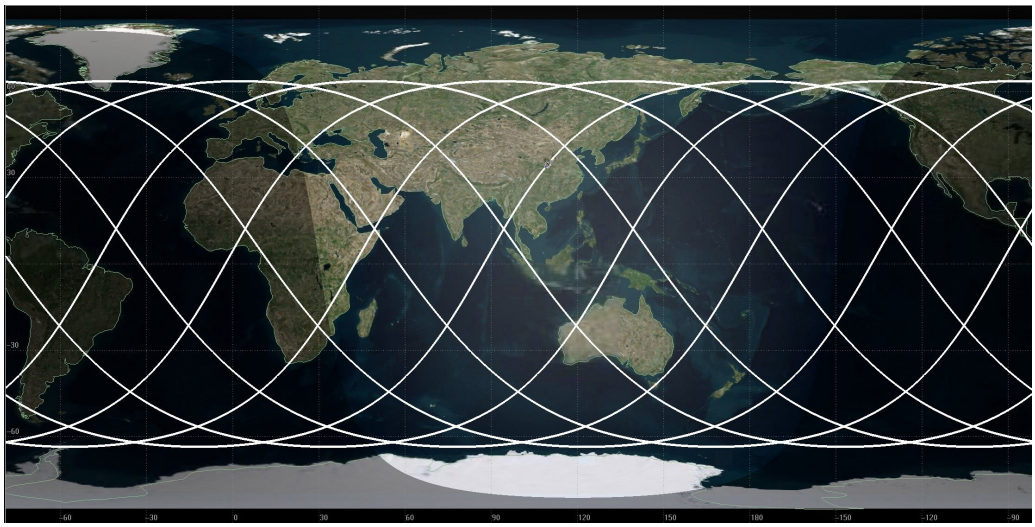


Figure 6. Ground track of a repeat orbit with eight revolutions per day.

The following is the Algorithm 1 process [24] to optimize the orbital semi-major axis. The iterative loop continues until the difference between a and a_{new} falls below a predefined convergence tolerance (e.g., $|a - a_{new}| \leq 10^{-6}$ km). By utilizing this numerical approach, the precise semi-major axis a that satisfies the repeating ground-track conditions for the required revisit frequency can be accurately determined.

Algorithm 1 Optimize the orbital semi-major axis

Input: $\mathrm{k_{RevPerDay}}$,e,i
Output: a

Initialization
$\mathrm{n} = \mathrm{k_{RevPerDay}} \cdot \omega_{\mathrm{e}}$
$\mathrm{a_{new}} = \left(\mu(\frac{1}{\mathrm{n}})^2\right)^{\frac{1}{3}}$
Loop
$\mathrm{a} = \mathrm{a_{new}}$
$\mathrm{p} = \mathrm{a}(1 - \mathrm{e}^2)$
$\dot{\Omega} = -\frac{3\mathrm{nJ_2}}{2}\left(\frac{\mathrm{R_e}}{\mathrm{p}}\right)^2 \cos(\mathrm{i})$
$\dot{\omega} = \frac{3\mathrm{nJ_2}}{4}\left(\frac{\mathrm{R_e}}{\mathrm{p}}\right)^2 (4 - 5\sin^2(\mathrm{i}))$
$\dot{\mathrm{M}}_0 = \frac{3\mathrm{nJ_2}}{4}\left(\frac{\mathrm{R_e}}{\mathrm{p}}\right)^2 \sqrt{1 - \mathrm{e}^2}\left(2 - 3\sin^2(\mathrm{i})\right)$
$\mathrm{n} = \mathrm{k_{RevPerDay}}\left(\omega_{\mathrm{e}} - \dot{\Omega}\right) - \left(\dot{\mathrm{M}}_0 - \dot{\omega}\right)$
$\mathrm{a_{new}} = \left(\mu(\frac{1}{\mathrm{n}})^2\right)^{\frac{1}{3}}$
END Loop

Using the aforementioned algorithm, the semi-major axis a that satisfies the revisit conditions (i.e., an orbit with a repeating ground track) can be determined. The apogee altitude H_a can then be calculated using the following equation:

$$H_a = 2a - 2r - H_p \tag{13}$$

3.4. Determination of the RAAN Ω

The right ascension of the ascending node can be calculated based on the local time of the ascending node and the longitude of the target region. The right ascension of the ascending node of the orbit is then determined using the following equation:

$$\Omega = \gamma - \arccos\left(\frac{\cos(\omega)}{\cos(i)}\right) \tag{14}$$

Through the above procedure, the full orbital parameters of the reference orbit are established: inclination i, semi-major axis a, eccentricity e, argument of perigee ω, and RAAN Ω. The resulting orbit is an elliptical critical Sun-synchronous repeat orbit, tailored for efficient and stable discontinuous regional coverage.

4. Constellation Configuration Design

At present, most common constellation configuration are developed for circular orbits [28], aiming to achieve global or quasi-global uniform coverage. These configurations typically adopt even angular spacing in both the orbital planes and the satellites themselves, resulting in highly regular, repeatable coverage patterns.

However, for elliptical orbit constellations, configuration design methods are relatively underdeveloped. The irregularity of the ground tracks and asymmetry in orbital velocity (due to eccentricity) pose challenges to straightforward replication of circular-orbit design rules. This paper proposes a dedicated configuration methodology for elliptical constellations, drawing partial inspiration from the Walker pattern but adapting it to fit the unique dynamics of elliptical return orbits.

Walker constellations are a design approach used to deploy satellites across multiple orbital planes [29]. The primary purpose of such constellations is to enhance regional or global coverage by evenly distributing satellites across these planes. This configuration minimizes overlap in satellite coverage, thereby improving the overall efficiency of the system. Walker constellation designs are typically characterized by three parameters: $N/P/F$, which also serve as the configuration description. N (Total number of satellites): This is the total number of satellites in the constellation, which primarily determines the scale of the constellation. It directly impacts the system's cost, coverage area, revisit frequency, and redundancy. P (Number of orbital planes): This represents the total number of different orbital planes to which the satellites are allocated. F (Phasing factor): This is the phase difference between satellites in adjacent orbital planes, that is, the angular difference between corresponding satellites in these planes.

Once the three parameters $N/P/F$ are determined, the satellite constellation configuration design is complete. Generally, it is challenging to directly specify the constellation's three configuration parameters. This paper presents a design method for the constellation configuration parameters aimed at intermittent observation of specific regions.

In the previous section, when designing the constellation's baseline orbit, a repeat orbit was adopted, and the orbital period T is given by the following expression:

$$T = 2\pi\sqrt{\frac{a^3}{GM}} \tag{15}$$

where a is the semi-major axis of the orbit and GM is the Earth's gravitational parameter. It is worth mentioning, in this paper, the period in Equation (15) is used as a reference repeating period for the construction of the constellation geometry. The orbit design and all numerical simulations are performed with a perturbation model, so that the actual nodal motion and ground-track evolution are accurately represented. Since it is a repeating orbit,

there exists a repeating factor k, meaning that after the baseline orbit satellite completes k revolutions around the Earth, its ground track begins to repeat. Here, we propose a $kn/kn/k$ constellation configuration design, corresponding to the constellation configuration parameters $N = kn$, $P = kn$, and $F = k$. In this formulation, n is the constellation design parameter, whose value is related to the intermittent observation time index t for the specific region; its specific relationship is provided in the following expression:

$$T = nt \tag{16}$$

With a fixed index t, the elliptical orbit constellation configurations under different orbital periods are shown in Table 1.

Table 1. Constellation configurations for different orbits under the same time index.

Time Index t	Repeating Factor k	Configurations $N/P/F$	Orbital Period T
1 h (3600 s)	12	24/24/12	2 h
	8	24/24/8	3 h
	6	24/24/6	4 h
	4	24/24/4	6 h

Here, the coverage area is chosen as Qinling, and the corresponding regional revisit period heatmap is shown in Figure 7. It illustrates the spatial distribution of revisit time over the target region for constellation configurations with orbital periods of 2 h, 3 h, 4 h, and 6 h. The color bar indicates the revisit time in seconds. All constellations are designed to achieve a theoretical revisit time of 3600 s (1 h). It can be observed that the revisit time across most of the target region is close to the theoretical value, demonstrating that the proposed design method effectively maintains the desired temporal resolution despite differences in orbital period. Minor deviations appear in some boundary areas, which can be attributed to geometric effects of the orbital configuration. Under the proposed configuration, the constellations with different orbital periods are all capable of achieving fixed-time revisits to the target region. Moreover, under a fixed time index t, the configuration parameters N and P of constellations with different orbital periods remain the same, with only F, i.e., the repeating factor k, varying.

With the constellation's baseline orbit altitude fixed (i.e., a fixed orbital period T), the theoretical time index t for different constellation configurations is shown in Table 2.

Table 2. Theoretical time index for different constellation configurations under the same orbit.

Orbital Period T	Configurations $N/P/F$	Theoretical Time Index t
3 h	16/16/8	1.5 h (5400 s)
	24/24/8	1 h (3600 s)
	32/32/8	0.75 h (2700 s)
	48/48/8	0.5 h (1800 s)

Here, Qinling is still selected as the coverage area, and its corresponding regional revisit period heatmap is shown in Figure 8. Revisit time distribution over the target region for constellations with different numbers of satellites, where all satellites operate in 3 h orbits. The subplots correspond to increasing satellite numbers, resulting in theoretical revisit times of 1.5 h, 1 h, 0.75 h, and 0.5 h, respectively. The color scale represents the revisit time in seconds. It can be observed that the achieved revisit time across the target region closely matches the theoretical values, while the spatial distribution becomes more uniform as the number of satellites increases. As shown in Figure 8, under a fixed orbital period, revisits at the theoretical time can be achieved by setting different configuration parameters.

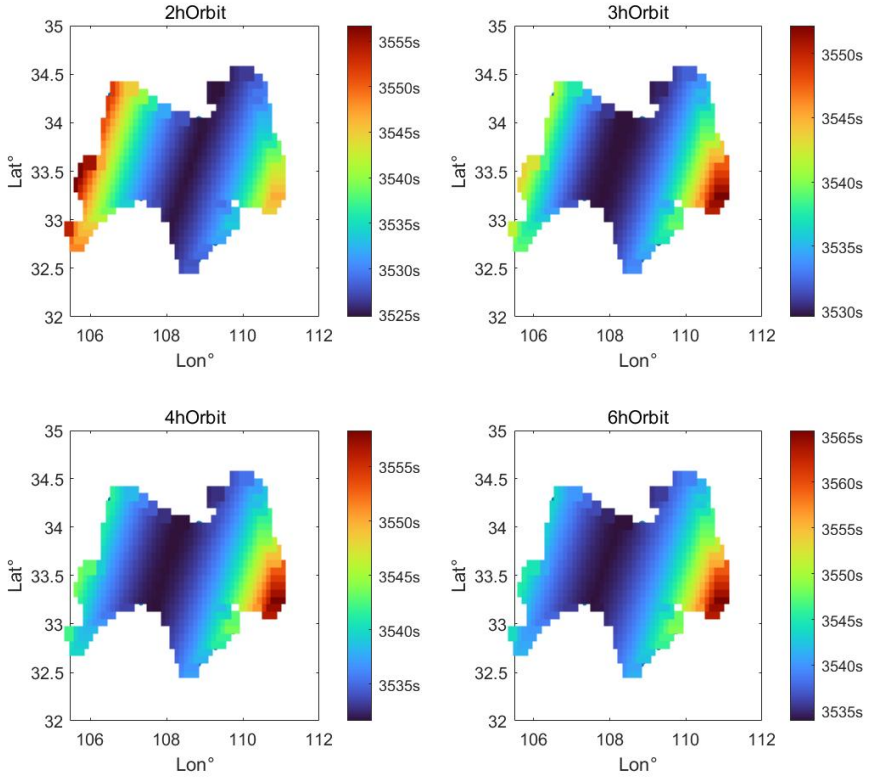


Figure 7. Coverage map with a 1 h revisit cycle.

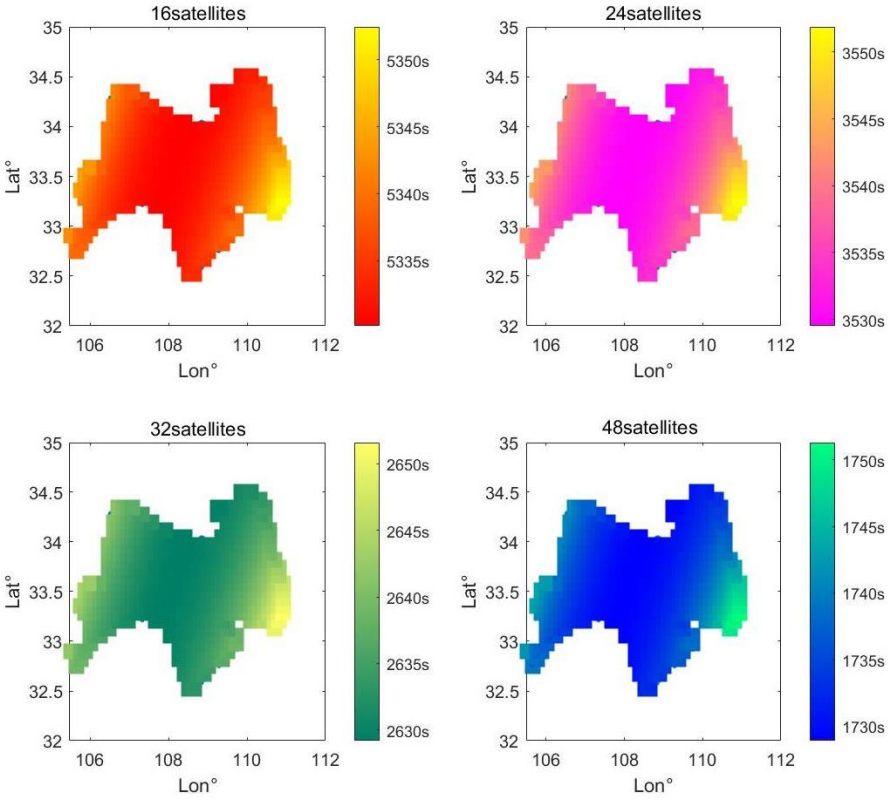


Figure 8. Coverage map with a 3 h orbital period.

These simulations validate the flexibility of the proposed $kn/kn/k$ design pattern, demonstrating how it can be tailored to meet specific temporal and spatial resolution requirements in regional observation missions.

The proposed configuration method enables systematic design of elliptical orbit constellations for regional observation tasks. By defining a time-based parameter n tied to revisit requirements, and introducing a structured approach to phasing and satellite allocation, this method provides a scalable framework for constellation planning. Combined with heatmap-based simulation validation, this design scheme can be extended to applications in wildfire monitoring, emergency response, and dynamic environmental observation.

5. Samples

This section presents a case study of a forest fire monitoring mission in the Qinling region, which applies the constellation design methodology discussed in earlier sections. The Qinling region, located in China, is critical for monitoring forest fires and environmental changes, requiring efficient satellite coverage for both temporal and spatial resolution.

The Qinling regions spans a latitude range of 33°30′ N to 35°20′ N and a longitude range of 105°30′ E to 110°15′ E. The coverage requirement for this mission is to access the target area every hour, corresponding to maximum revisit period of 3600 s. In other words, the time index t is 1 h.

First, apply the orbital design methodology described in Section 3 to design the reference orbit for the constellation. A critical elliptical Sun-synchronous repeat ground track orbit is selected for this purpose, with specific steps following the guidelines outlined in Section 3. The designed parameters of the reference orbit are listed in Table 3.

Table 3. Parameters of the reference orbit.

Apogee Altitude	Perigee Altitude	Inclination Angle	Argument of Perigee	RAAN	Mean Anomaly
8065.65 km	300 km	116.565°	141°	155°	0°

Using the orbital period formula, the reference orbit period T is calculated as 10,801 s (180.0167 min), and constellation configuration design methodology introduced in the previous section, the parameter n can be derived using the time index t and orbital period T. The resulting constellation configuration parameters are (24/24/8), indicating: a total of 24 satellites, distributed across 24 orbital planes (1 satellite per plane), with a phasing factor of 8. The ground tracks and spatial distribution of this constellation are illustrated in the figures below.

For Figures 9–11, the orbit is propagated in STK with the J_2-only dynamics model, i.e., including the Earth's central gravity and the J_2 oblateness term, without atmospheric drag or higher-order geopotential harmonics. The perturbation models adopted in this study differ according to the objective of each analysis stage. In the frozen-orbit derivation, the J_2 and J_3 zonal harmonics are included because the frozen-orbit condition is primarily determined by their combined effect on the secular evolution of the orbital elements. In contrast, the constellation propagation and coverage verification shown in Figures 9 and 10 are performed using a J_2-only model, since this part focuses on short-term repeating-ground-track characteristics and revisit-performance evaluation, for which J_2 is the dominant perturbation. Atmospheric drag is considered separately in the lifetime analysis of Section 2.1, where long-term orbital decay is the key issue, but is not included in the short-term coverage simulations. Therefore, different model fidelities are adopted intentionally according to the specific purpose of frozen-orbit design, revisit verification, and lifetime assessment.

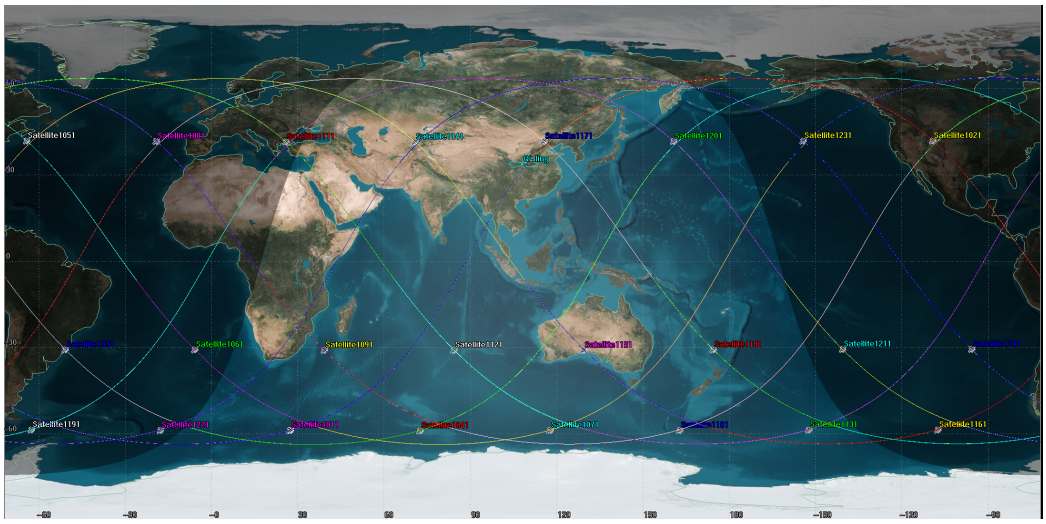


Figure 9. The ground tracks of the designed constellation.

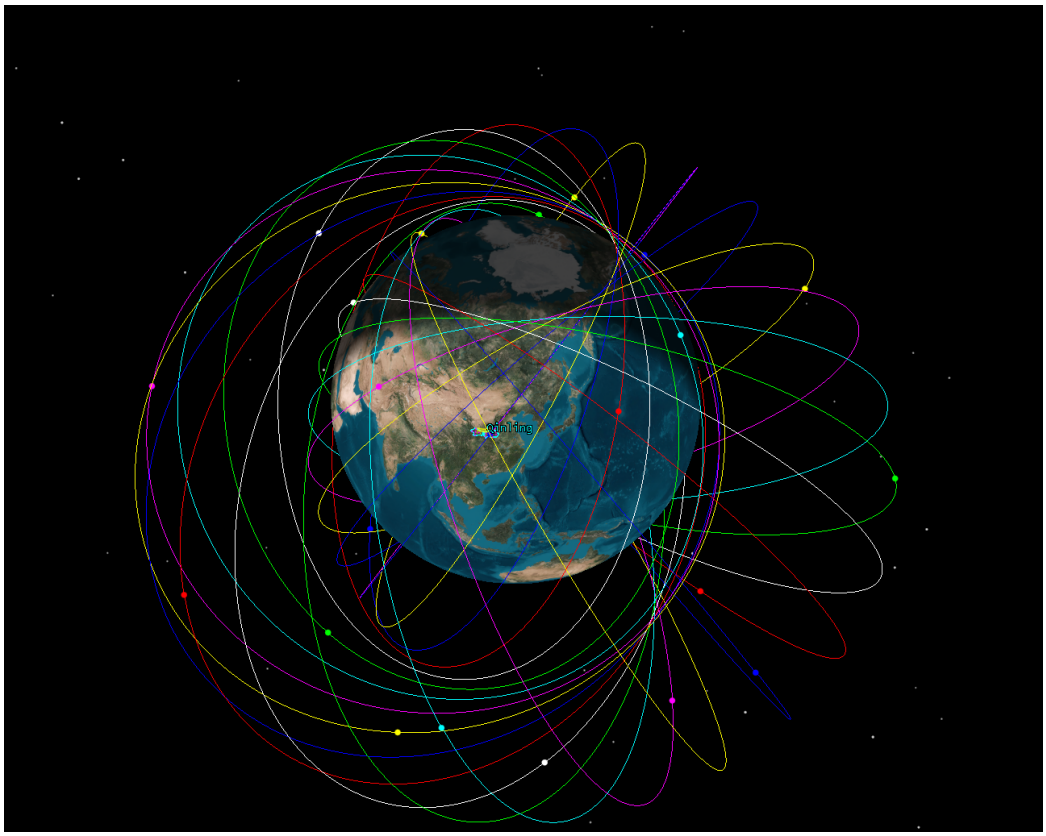


Figure 10. The spatial distribution of the designed constellation.

The maximum revisit time for the target area is calculated and shown in Table 4, based on the satellite's ground track configuration. The table presents the revisit time for each longitude across the target area, calculated for the 24/24/8 constellation configuration.

It should be noted that the revisit-time evaluation was not conducted only at the five longitude points reported in Table 4. In fact, the entire Qinling target region was discretized into a dense grid with a spatial resolution of $0.1^\circ \times 0.1^\circ$, and the revisit time was calculated for all grid points within the region. For concise presentation, Table 4 only lists representative results obtained from several selected longitude sections, where the reported values correspond to the averaged revisit-time performance along these longitudes. Therefore, the results in Table 4 are intended as a compact statistical representation rather than a sparse pointwise validation. As calculated from Table 4, the maximum revisit

time across the target area is within 3600 s, thereby meeting the requirement for an hour revisit cycle.

Table 4. Maximum revisit time at each longitude for the target area with designed constellation.

Longitude°	Revisit Time s
106	3595
107	3580
108	3577
109	3579
110	3583

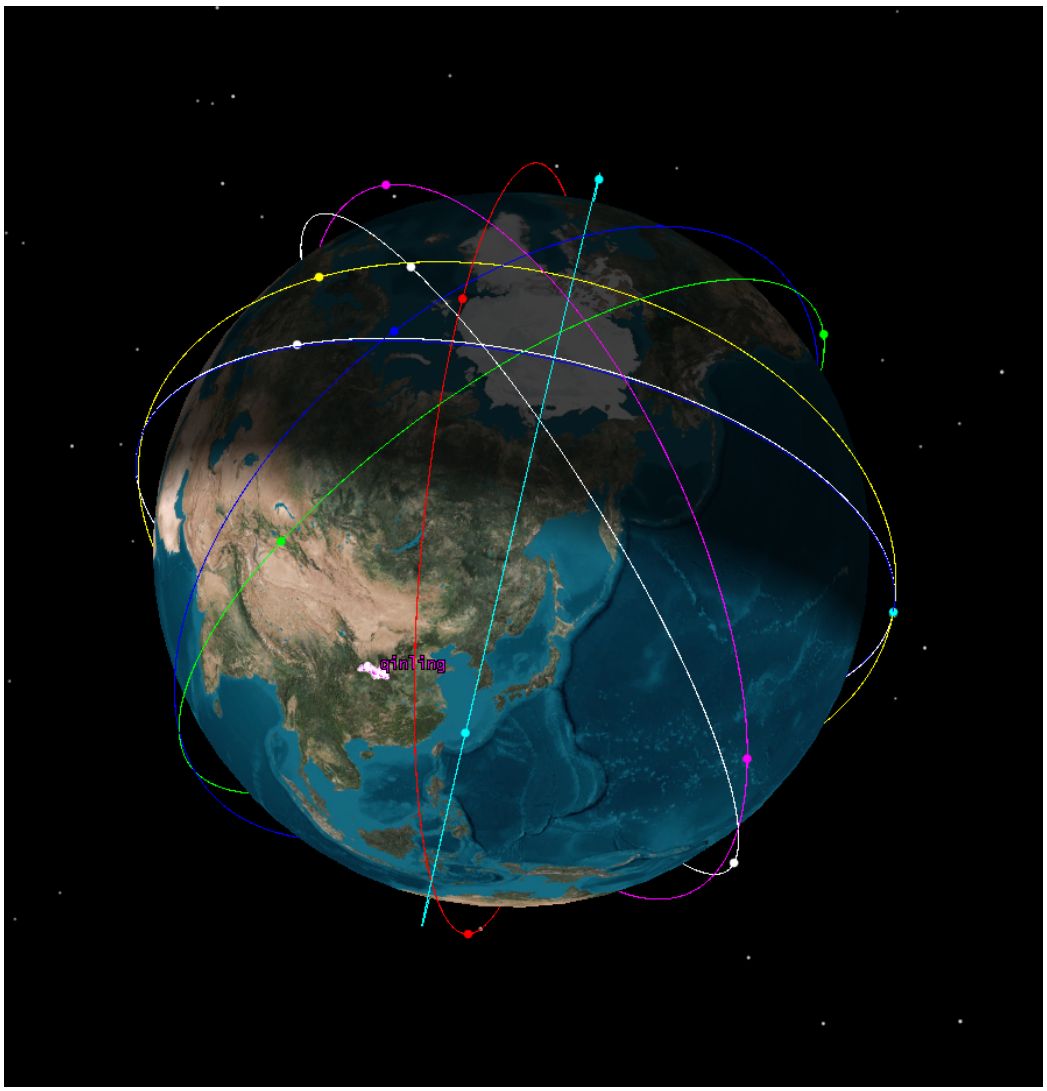


Figure 11. The spatial distribution of Walker.

To provide a more direct comparison with a conventional circular-orbit constellation, a 24-satellite Walker constellation in a 500 km Sun-synchronous circular orbit is constructed for the Qinling regional observation mission. The configuration parameters of the Walker are (24/8/3), indicating: a total of 24 satellites, distributed across 8 orbital planes (3 satellites per plane), with a phasing factor of 3. The spatial distribution of this constellation is illustrated in Figure 11. The maximum revisit time for the target area is calculated and shown in Table 5. The simulation results show that the maximum revisit time of this Walker constellation is approximately 8200 s, which is significantly larger than the target

revisit requirement of 1 h (3600 s). By contrast, the proposed elliptical constellation satisfies the 1 h revisit requirement with the same number of satellites. This comparison further demonstrates the advantage of the proposed elliptical constellation for discontinuous regional coverage missions, especially in terms of revisit performance under the same constellation scale.

Table 5. Maximum revisit time at each longitude for the target area with Walker.

Longitude°	Revisit Time s
106	8264
107	8273
108	8270
109	8265
110	8270

Figure 12 illustrates the coverage statistics:

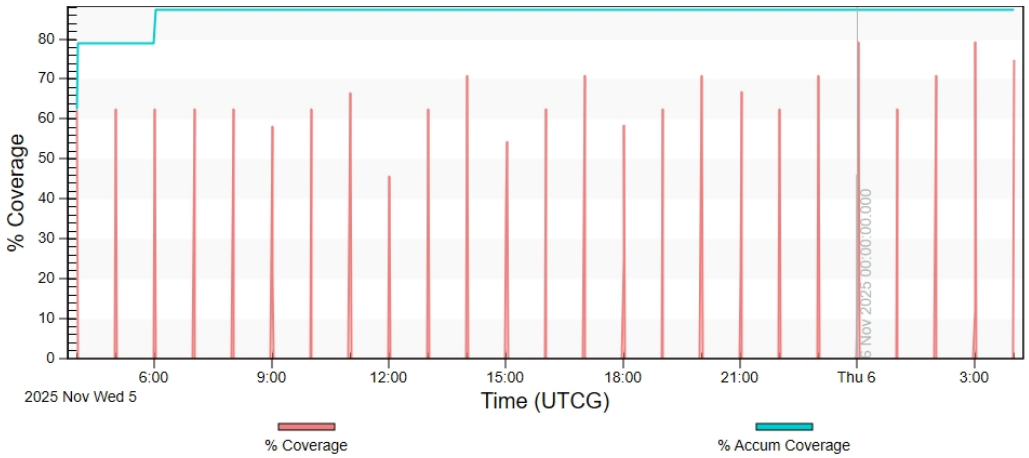


Figure 12. Temporal variation of regional coverage percentage for the designed constellation.

In Figure 12, the red bars denote the instantaneous coverage percentage over the target area, while the blue line represents the accumulated coverage ratio. The red bar represents the instantaneous coverage percentage, which shows the real-time coverage of the region at any given moment. The coverage fluctuates periodically throughout the time period, indicating the periodic nature of satellite passes over the target area. The blue line represents the cumulative coverage percentage, which increases steadily over time, showing the total coverage achieved by the constellation. The cumulative coverage rises toward a plateau, reflecting the constellation's ability to progressively cover the region as satellites repeatedly pass over it. Despite the periodic fluctuations, the satellite constellation provides high and stable coverage over time, achieving nearly 80 percent coverage of the target region. This indicates the constellation's high efficiency in regional observation tasks.

6. Conclusions

This paper presents a detailed comparison of low-Earth circular orbits and elliptical orbits, specifically focusing on their application in regional observation remote sensing tasks. While circular orbits are effective for global coverage, they are less efficient for targeted regional observations that require frequent access to specific areas. Elliptical orbits, on the other hand, provide a distinct advantage for such tasks, as they can focus coverage on hotspot regions, ensuring rapid revisit and high spatial resolution.

To achieve optimal performance while minimizing orbital maintenance costs, we selected a highly elliptical orbit design. By utilizing a frozen orbit configuration (i.e., a critical

inclination orbit), we ensured stable perigee positioning, reducing the need for frequent station-keeping. This configuration is especially beneficial for long-term missions, such as forest fire monitoring, where consistent satellite passes over specific regions are crucial. Additionally, the Sun-synchronous repeat ground track orbit was adopted to ensure predictable, consistent observation of the target region.

Subsequently, the paper details a systematic workflow to derive specific orbital parameters based on the target mission area, outlining how to design a critical elliptical Sun-synchronous repeat ground track orbit. With the reference orbit established, the study introduces a constellation design methodology. The mathematical relationships between constellation configuration parameters and coverage metrics are established to guide the design process. Finally, through a case study simulating the Qinling forest fire monitoring mission, the paper presents the orbital and constellation configuration parameters deter-mined by the proposed method. Simulation results confirm that the constellation's coverage characteristics meet predefined requirements, demonstrating the effectiveness of the design framework.

In conclusion, the proposed elliptical orbit constellation design is a crucial advancement for regional observation remote sensing tasks, where high-frequency revisit and long operational duration are essential. The method provides an efficient, cost-effective solution for monitoring hotspot regions, ensuring that satellites can achieve near real-time observation over critical geographic areas. Future work will focus on the operational sustainment of these specific geometries in complex perturbation environments. Specifically, applying control barrier functions to satellite constellation configuration maintenance control presents a promising theoretical avenue for safely and efficiently preserving these local area observation capabilities over the extended mission lifetime. In addition, the robustness of the proposed constellation under satellite failure is an important practical issue. Since the nominal configuration considered in this paper contains one satellite per orbital plane, the loss of a single satellite may disrupt the designed phasing relationship and reduce revisit uniformity over the target region. Nevertheless, such a failure would generally lead to performance degradation rather than a complete loss of regional observation capability. The actual impact would depend on the failed orbital position, the temporal observation requirement, and the spatial distribution of the target area. Possible robustness-enhancement strategies, such as in-orbit spare deployment, redundant plane design, or post-failure phase reconfiguration, are not considered in the present study and will be investigated in future work.

Author Contributions: Conceptualization, Y.W. and Z.Z.; methodology, Y.W. and Z.Z.; software, Y.W.; validation, Y.W. and Z.Z.; formal analysis, Y.W.; investigation, Y.W.; resources, Z.Z.; data curation, Y.W.; writing—original draft preparation, Y.W.; writing—review and editing, Y.W. and Z.Z.; visualization, Y.W.; supervision, Z.Z.; project administration, Y.W.; funding acquisition, Z.Z. All authors have read and agreed to the published version of the manuscript.

Funding: This research received no external funding.

Data Availability Statement: The raw data supporting the conclusions of this article will be made available by the authors upon request.

Conflicts of Interest: The authors declare no conflicts of interest.

References

1. Lagunas, E.; Chatzinotas, S.; Ottersten, B. Low-Earth orbit satellite constellations for global communication network connectivity. *Nat. Rev. Electr. Eng.* **2024**, *1*, 656–665. [CrossRef]
2. Li, Y.; Wang, M.; Hwang, K.; Li, Z.; Ji, T. LEO Satellite Constellation for Global-Scale Remote Sensing With On-Orbit Cloud AI Computing. *IEEE J. Sel. Top. Appl. Earth Obs. Remote Sens.* **2024**, *16*, 9369–9381. [CrossRef]
3. Yang, Y.; Mao, Y.; Ren, X.; Jia, X.; Sun, B. Demand and key technology for a LEO constellation as augmentation of satellite navigation systems. *Satell. Navig.* **2024**, *5*, 11. [CrossRef]

4. Huang, S.; Colombo, C.; Bernelli-Zazzera, F. Multi-criteria design of continuous global coverage Walker and Street-of-Coverage constellations through property assessment. *Acta Astronaut.* **2021**, *188*, 151–170. [CrossRef]
5. Soung, S.L.; Jong, P.K.; Eungnoh, Y.; Jae-Hyuk, Y.; Ho-Hyun, S. Satellite constellation method to achieve desired revisit performance for multiple targets. *J. Appl. Remote Sens.* **2024**, *18*, 024509 . [CrossRef]
6. Walker, J.G. Satellite constellations. *J. Br. Interplanet. Soc.* **1984**, *37*, 559.
7. Beste, D. Design of satellite constellations for optimal continuous coverage. *IEEE Trans. Aerosp. Electron. Syst.* **1978**, *14*, 466–473. [CrossRef]
8. Zhang, T.-J.; Shen, H.-X.; Li, Z.; Qie, H.; Cao, J.; Li, H.-N.; Yang, Y.-K. Restricted constellation design for regional navigation augmentation. *Acta Astronaut.* **2018**, *150*, 231–239. [CrossRef]
9. Lee, S.S. Explicit mathematical formulation and coverage consistency of satellite constellation designs for repeating ground track orbits. *IEEE Trans. Aerosp. Electron. Syst.* **2024**, *60*, 1102–1112. [CrossRef]
10. Casanova, D.; Avendaño, M.E.; Mortari, D. Design of flower constellations using necklaces. *IEEE Trans. Aerosp. Electron. Syst.* **2014**, *50*, 1347–1358. [CrossRef]
11. He, X.; Gao, X.; Bao, L.; Shao, S.; Jia, G. Restricted 2D Necklace Flower Constellation Design Theory for Discontinuous Coverage. *IEEE Trans. Aerosp. Electron. Syst.* **2025**, *61*, 13202-13212. [CrossRef]
12. Ferreira, L.S.; Casanova, D.; Tresaco, E.; Prado, A.F.B.A. Satellite constellation design for Titan exploration: Orbit design and performance assessment. *Satell. Navig.* **2025**, *6*, 27. [CrossRef]
13. Ulybyshev, Y.A. General analysis method for discontinuous coverage satellite constellations. *J. Guid. Control. Dyn.* **2015**, *38*, 2475–2483. [CrossRef]
14. He, X.; Li, H. General analysis method for global revisit characteristics of satellite constellation with repeating ground tracks. *Acta Astronaut.* **2023**, *202*, 319–332. [CrossRef]
15. Deccia, C.M.A.; Wiese, D.N.; Nerem, R.S. Using a multiobjective genetic algorithm to design satellite constellations for recovering Earth system mass change. *Remote Sens.* **2022**, *14*, 3340. [CrossRef]
16. Razoumny, Y.N. Route satellite constellations for Earth discontinuous coverage and optimal solution peculiarities. *J. Spacecr. Rocket.* **2017**, *54*, 572–581. [CrossRef]
17. Sarno, S.; De Graziano, M.; D'Errico, M. Polar constellations design for discontinuous coverage. *Acta Astronaut.* **2016**, *127*, 367–374. [CrossRef]
18. Lee, S.S. Satellite constellation method for ground targeting optimized with k-means clustering and genetic algorithm. *Eng. Appl. Artif. Intell.* **2024**, *129*, 107509. [CrossRef]
19. Tang, X.; Xu, Y.; Huang, L.; Ning, Q.; Ullah, H. A multiarea on-demand classification constellation design for satellite IoT. *IEEE Internet Things J.* **2024**, *11*, 23889–23905. [CrossRef]
20. Mencarelli, L.; Floquet, J.; Georges, F. Matheuristics approaches for the satellite constellation design problem. *Optim. Eng.* **2024**, *25*, 1051–1067. [CrossRef]
21. Razoumny, Y.N. Fundamentals of the route theory for satellite constellation design for Earth discontinuous coverage. Part 2: Synthesis of satellite orbits and constellations *Acta Astronaut.* **2016**, *128*, 741–758. . [CrossRef]
22. Kim, D.Y.; Chung, T.J. Design of an elliptical orbit for high-resolution optical observation at a very low altitude over the Korean Peninsula. *J. Astron. Space Sci.* **2023**, *40*, 35–43. [CrossRef]
23. King-Hele, D.G. *Satellite Orbits in an Atmosphere: Theory and Applications*; Blackie: Glasgow, UK, 1987.
24. Vallado, D.A. *Fundamentals of Astrodynamics and Applications* ; Microcosm Press: Hawthorne, CA, USA, 2013.
25. Wertz, J.R. *Mission Geometry: Orbit and Constellation Design and Management*; Microcosm Press: El Segundo, CA, USA; Kluwer Academic Publishers: Dordrecht, The Netherlands , 2001.
26. Gong, Y.P. Research on Configuration Design and Coverage Analysis Method of Low-Orbit Giant Constellation. Harbin. 2022. Available online: https://d.wanfangdata.com.cn/thesis/D02779307 (accessed on 2 November 2022).
27. Ouyang, Y.; Feng, T.; Wei, Y.; Zheng, J.; Sun, C.; Zhang, H. A constellation design method for forest fire monitoring. In *Proceedings of SPIE 13565, Earth Observing Systems 2025*; SPIE: Bellingham, WA, USA, 2025; Volume 13565, pp. 1356512–1356518. [CrossRef]
28. Ruan, Y.J.; Hu, M.; Yun, Z.M. Research progress and prospects of low-orbit mega-constellation configuration design and control. *China Space Sci. Technol.* **2022**, *42*, 1–15. [CrossRef]
29. Walker, J.G. Some circular orbit patterns providing continuous whole earth coverage. *J. Br. Interplanet. Soc.* **1970**, *24*, 369–384.

Disclaimer/Publisher's Note: The statements, opinions and data contained in all publications are solely those of the individual author(s) and contributor(s) and not of MDPI and/or the editor(s). MDPI and/or the editor(s) disclaim responsibility for any injury to people or property resulting from any ideas, methods, instructions or products referred to in the content.